Applied Surface Science 496 (2019) 143527

Contents lists available at ScienceDirect

Applied Surface Science

journal homepage: www.elsevier.com/locate/apsusc

Full length article

Thermal diffusion and epitaxial growth of Ag in $Ag/SiO_2/Si$ probed by XRD, depth-resolved XPS, and slow positron beam

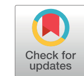

J.D. Liu[a,b], Z.W. Liu[c], Z.Q. Chen[c], H.J. Zhang[a,b,*], B.J. Ye[a,b,*]

[a] State Key Laboratory of Particle Detection and Electronics, University of Science and Technology of China, Hefei 230026, China
[b] Hefei National Laboratory for Physical Sciences at the Microscale, University of Science and Technology of China, Hefei 230026, China
[c] Hubei Nuclear Solid Physics Key Laboratory, Department of Physics, Wuhan University, Wuhan 430072, China

ARTICLE INFO

Keywords:
$Ag/SiO_2/Si$
Multilayer
Epitaxial growth
Positron beam

ABSTRACT

$Ag/SiO_2/Si$ multilayer samples with different SiO_2 layer thicknesses were prepared through deposition of Ag layer onto SiO_2/Si substrates at different substrate temperatures (T_{sub}) by RF magnetron sputtering method. Microstructure of the multilayer was characterized by XRD $\theta/2\theta$ scan and φ-scan analysis, depth-resolved XPS analysis, and Doppler broadening of annihilation radiation (DBAR) spectra of positron measurements. The experimental results indicate that, at T_{sub} = 25 °C, the Ag deposition forms $Ag/SiO_2/Si$ multilayer structure. With T_{sub} increasing to 200 °C, Ag atoms are found to diffuse into the SiO_2 layer. This thermal diffusion process plays a critical role in removing SiO_2 layer on the Si substrate. At T_{sub} of 600 °C, the 31-nm-thick SiO_2 layer is partially desorbed from the Si surface as a result of Ag diffusion, and eventually results in a deposition of Ag layer directly on the Si substrate. This is also confirmed by the XRD φ-scan measurements, which indicates epitaxial growth of Ag atoms directly on the surface of Si substrate at T_{sub} of 600 °C.

1. Introduction

The metal/Si systems have attracted tremendous attention due to the potential applications of their electronic [1], magnetic, optical properties [2], and in fundamental mechanic growth process [3, 4]. Among all metal/Si systems, Ag/Si is one of the most interesting subjects due to its non-interactive and atomically abrupt interface [5], also for the smallest electrical resistivity by Ag and the most practically used substrate of Si(001) [6-8]. In the past decade, it is well known that epitaxial growth of silver on silicon can be obtained by evaporation techniques such as molecular beam epitaxy [9, 10]. However, traditional epitaxial growth requires clean Si substrate surface, and thermal annealing at high temperature in ultrahigh vacuum condition.

In recent years, a new mechanism was proposed that during magnetron sputtering process [11-13], the bombardment of highly energetic sputtered particles with the outmost oxide layer enables desorption of the oxide layer from Si substrate surface, and thus allows foreign atoms to reach the Si surface [4]. So the presence of a thin SiO_2 layer has been utilized for the benefit of growing epitaxial Ag film on Si. Obviously, structural defects and incomplete growth residues at interface will highly affect the quality of deposited overlayer. It is thus quite important to probe the interfaces buried at certain depth in the $Ag/SiO_2/Si$ multilayer and to identify the type and the concentration of structural defects [14]. However, very few methods can give direct identification of atomic-scaled defects and also provide depth-resolved analysis of the defect distribution.

Positron is a unique probe for the nanometer-scaled defects in materials. By changing the incident energy of the positron beam, positron implantation depth in the sample can be controlled, and the depth distribution of defects near the subsurface area can be obtained. A high-purity Ge detector was used to collect the annihilation γ-rays to construct the Doppler broadening of annihilation radiation (DBAR) spectroscopy. S parameter is used to characterize the DBAR spectrum, which is defined as the ratio of the annihilation events in the central region (511 ± 0.76 keV) of the 511 keV annihilation peak to the total number of counts within the peak. Thus, when positrons are trapped at low electron density environment such as vacancies, they have less chance to annihilate with high momentum core electrons, leading to a narrower DBAR spectra [15, 16]. For this reason, an S parameter larger than the defect-free bulk value is often associated with vacancy-type defects and, in many cases, it can also provide information on the local chemical environment where positrons annihilate [17-21]. Furthermore, $Ag/SiO_2/Si$ multilayer is an interesting system since it benefits from the following factors: (1) Positron affinity of Ag is rather strong in transition metals [22-27] so that a positron prefers to annihilate with Ag; (2) The S parameter in SiO_2 and Si is relatively higher than that in

* Corresponding authors at: State Key Laboratory of Particle Detection and Electronics, University of Science and Technology of China, Hefei 230026, China.
E-mail addresses: hjzhang8@ustc.edu.cn (H.J. Zhang), bjye@ustc.edu.cn (B.J. Ye).

https://doi.org/10.1016/j.apsusc.2019.07.269
Received 26 March 2019; Received in revised form 24 June 2019; Accepted 29 July 2019
Available online 02 August 2019
0169-4332/ © 2019 Published by Elsevier B.V.

Ag; (3) The diffusion length of positron in SiO_2 is very short (less than 10 nm), while in Si single crystal the diffusion length is much longer (commonly in the range of 100 nm). In this work, we utilize a mono-energetic positron beam to investigate the diffusion of Ag into SiO_2/Si at different T_{sub} during magnetron sputtering.

2. Experiment

2.1. Samples preparation

The SiO_2[31]/Si and SiO_2[110]/Si (the number in square brackets denotes layer thickness in nm) substrates were obtained by annealing the Si(001) wafers (10×10 mm) at 800 °C in an O_2 (99.999%) atmosphere. The 30-nm-thick Ag films were grown on SiO_2/Si substrates at different T_{sub} by RF magnetron sputtering method using an Ag (99.99%) target. The base pressure of deposition chamber is up to 3×10^{-6} Pa. During sputtering process, the pressure of working gas Ar (99.999%) was kept at 0.3 Pa. We denote samples in the way of Ag[30]/SiO_2[31]/Si@25 °C, where the temperature after @ denotes T_{sub} in °C.

2.2. XRD θ/2θ scan and φ-scan measurements

XRD measurements were performed on a high-resolution X-ray diffractometer (SmartLab, Rigaku) by using the X-rays from Cu K_α radiation. For XRD $\theta/2\theta$ measurements, the scanning range was from 20° to 90° with a step of 0.01°. The XRD φ-scan measurements were also performed on Si(001), Ag[30]/SiO_2[31]/Si@25 °C and 600 °C. In the φ-scan for Si(001) substrate, the 2θ angle was fixed at $2\theta = 28.443°$ and the tilt angle φ ranged from 40° to 80° with a step of 1°. While in the φ-scan for Ag film, the 2θ angle was fixed at $2\theta = 44.279°$ and the φ angle ranged from 40° to 80° with a step of 1°.

2.3. Depth-resolved XPS measurements

The depth-resolved XPS measurements were performed by using a PHI-5000 VersaProbe II (ULVAC-PHI, Chigasaki) system. The base vacuum level of the system is 2–3 × 10^{-8} Pa. During the depth-resolved measurements, the vacuum gets worse to 3–5 × 10^{-7}Pa. After each sputtering process (4 keV Ar^+ for 30 s), XPS analysis was carried out to quantitatively determine the atomic concentrations of all elements.

2.4. DBAR measurements

The DBAR measurements were carried out by using a magnetically guided variable-energy positron beam (0.2 –20.2 keV). For the convenience of comparison, all S parameters were normalized to the defect-free Si bulk value (*i.e.* S value of bulk Si equates to 1). To further understand the positron annihilation characteristics in Ag/SiO_2/Si, the VEPFIT [28] software has been employed to resolve the defect depth profiles and depth structures of deposited Ag/SiO_2/Si layers. The S parameter measured at different positron energy E is a linear combination of the specific S value for each layer. It can be formulated in the form of:

$$S(E) = S_s F_s(E) + \sum_{i=1}^{n} S_i F_i(E),$$

where S_s and S_i are the S parameters at surface and in ith layer, respectively, while F_s and F_i denote the fraction of positrons ($F_s(E) + \sum_{i=1}^{n} F_i(E) = 1$) annihilated at surface and in each layer, respectively. By considering the one-dimensional diffusion equation of positrons and the Makhov implantation profile using VEPFIT program, the S parameters and positron diffusion length in each layer can be obtained.

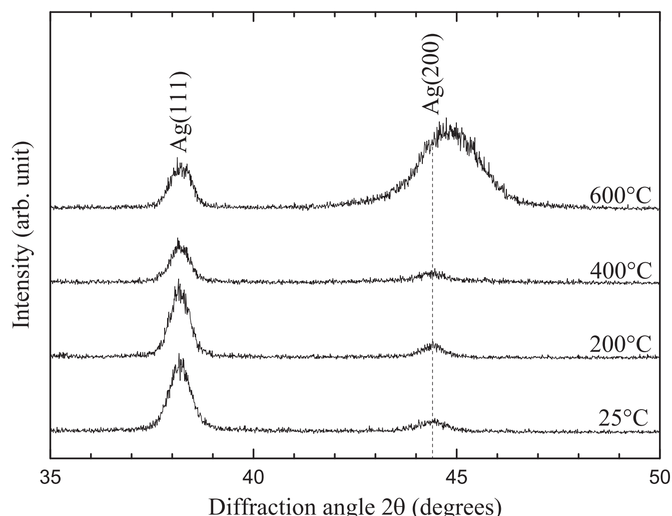

Fig. 1. XRD $\theta/2\theta$ diffraction patterns of Ag[30]/SiO_2[31]/Si @25, 200, 400, and 600 °C.

3. Results and discussion

3.1. XRD θ/2θ scan and φ-scan measurements

The XRD $\theta/2\theta$ scan profiles of Ag[30]/SiO_2[31]/Si@25, 200, 400, and 600 °C are shown in Fig. 1. It was found that, at T_{sub} = 25 °C Ag film was deposited and grown preferentially with (111) crystallographic direction and also exhibited meagre intensity of (200) reflection. With increasing T_{sub}, the intensity of (111) reflection peak becomes weaker while the intensity of (200) reflection peak becomes stronger. Most significantly, the dominant (111) peak intensity decreases with increasing (200) peak intensity at 600 °C. This change of Ag film orientation indicates that the mechanism of Ag film growth might have changed at elevated T_{sub}.

Fig. 2a–c shows the φ-scans of Si(001) wafer, Ag[30]/SiO_2[31]/Si@25 °C, and Ag[30]/SiO_2[31]/Si@600 °C, respectively. In Fig. 2b, the Ag (200) pole figure of Ag[30]/SiO_2[31]/Si@25 °C shows random growing orientation in all the directions. On the contrary, the Ag(200) pole figure of Ag[30]/SiO_2[31]/Si@600 °C reveals a remarkable fourfold symmetry and matches Si(111) poles well, which indicates the epitaxial relationship of Ag(110)/Si(110). The four distinct equidistant maximum pole densities were observed at the tilt angle φ of 54.7° which corresponds to the angle between the (111) and (001) planes in cubic crystals. It should be mentioned that this Ag film is initially sputtered onto SiO_2/Si substrate. However, in Ag[30]/SiO_2[31]/Si@600 °C, the O 1s peak becomes much weaker and narrower, and it can be seen clearly that the peak center of O 1s moves outward towards the surface. This suggests that SiO_2 is partially absorbed.

3.2. Depth-resolved XPS measurements

The depth profiles of atomic concentrations of all elements of SiO_2[31]/Si substrate, Ag[30]/SiO_2[31]/Si@25 °C, and Ag[30]/SiO_2[31]/Si@600 °C are shown in Fig. 2 (d), (e), and (f), respectively. In both SiO_2[31]/Si substrate and Ag[30]/SiO_2[31]/Si@25 °C, the different layers could be clearly observed from depth-resolved XPS. However, in Ag[30]/SiO_2[31]/Si@600 °C, no clear interface between the neighboring layers was observed. The XPS analysis shows that the deposited Ag atoms were diffused into the SiO_2 layer, and even a few percent of Ag atoms reached the Si layer.

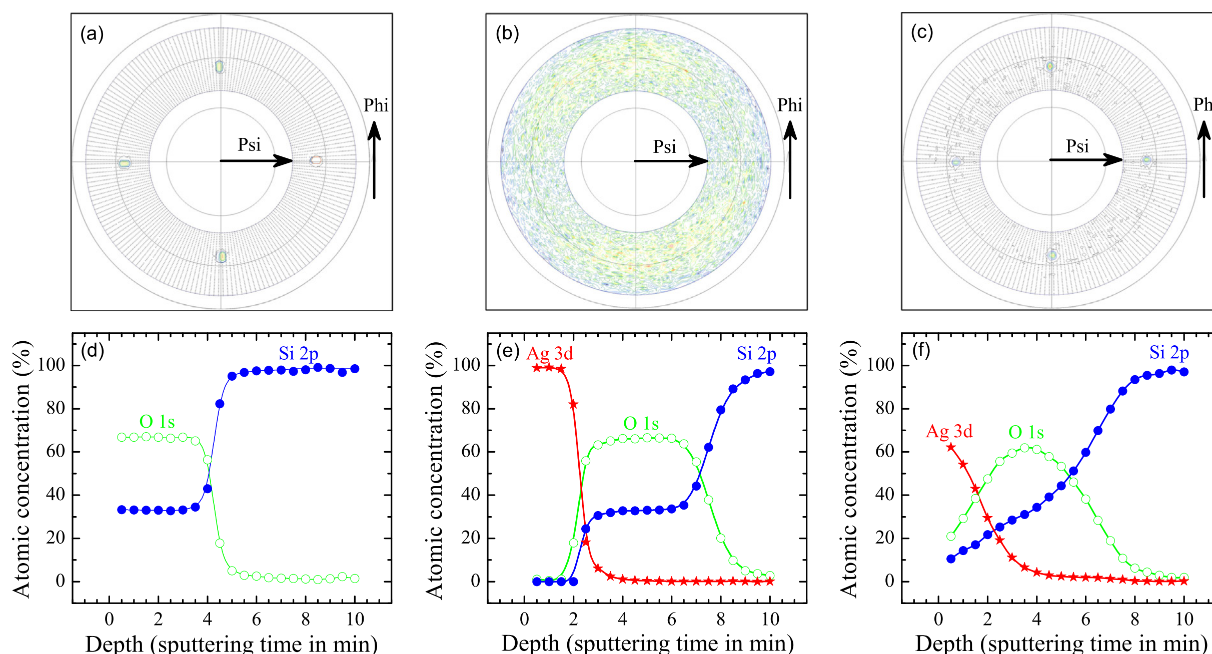

Fig. 2. (a) The Si(111) pole figure of Si(001) wafer. The Ag(200) pole figures of (b) Ag[30]/SiO_2[31]/Si@25 °C, and (c) Ag[30]/SiO_2[31]/Si@600 °C. Depth profiles of Ag, O, and Si concentrations of (d) SiO_2[31]/Si substrate, (e) Ag[30]/SiO_2[31]/Si@25 °C, and (f) Ag[30]/SiO_2[31]/Si@600 °C derived from depth-resolved XPS analysis.

3.3. DBAR measurements

The Doppler broadening S parameter, as a function of incident positron energy (S-*E* curve), for two types of SiO_2/Si samples with and without Ag deposition, are shown in Fig. 3, The solid lines are derived from VEPFIT fitting. In the S-*E* curve of SiO_2[110]/Si, there is a dip at around 3 keV which is identified as the SiO_2/Si interface [17-19]. When positron incident energy is lower than 3 keV, positrons mainly annihilate in the outmost SiO_2 layer. As incident energy increased, positrons can inject into Si substrate and diffuse in Si substrate in random-walk mode. Due to the attractive potential of the interface, some fraction of positrons stopped near this area can get trapped and annihilate at the interface. At SiO_2/Si interface, the S parameter is smaller than that in Si bulk or oxide. Generally, in a defective solid, the S value is expected to be higher than the bulk value in defect-free case. The lower S parameter than that of either Si or SiO_2 bulk is probably due to the change of electron momentum detected by positrons. In case of positron annihilation with core electrons of oxygen, there will be a substantial decrease of S parameter [29] At SiO_2/Si interface region, there are many dangling bond sites [30, 31]. Positrons are trapped at these sites, and annihilate with outer core-electrons of oxygen atoms, leading to a wider Doppler broadening peak and a lower S parameter [20]. However, in SiO_2[31]/Si, such similar interface was not detected by the positron beam. The 31-nm-thick SiO_2 layer is very thin (the interface is too shallow below the SiO_2 surface), and the surface state could compete with the SiO_2/Si interface, therefore the SiO_2/Si interface is difficult to be distinguished. Up to now, no such shallow interface in the SiO_2[31]/Si system has been detected by positron beam.

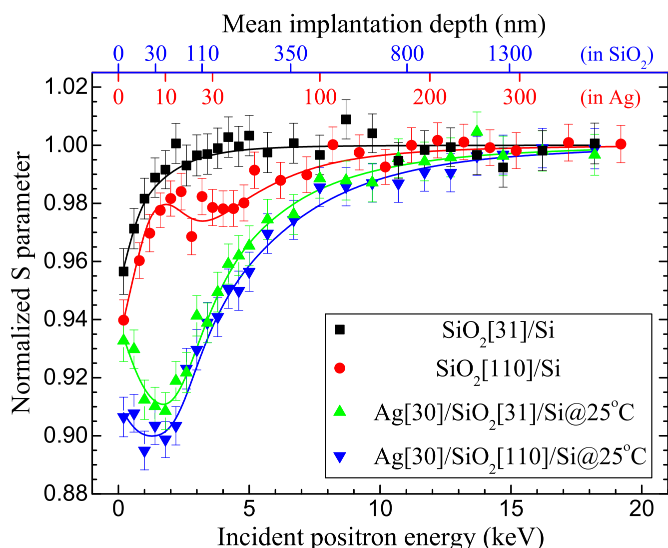

Fig. 3. Normalized S parameter as a function of incident positron energy for SiO_2[31]/Si, SiO_2[110]/Si, Ag[30]/SiO_2[31]/Si@25 °C, and Ag[30]/SiO_2[110]/Si@25 °C. The scatters are derived from the fitting by VEPFIT. The solid lines are eye-guide lines.

As shown in Fig. 3, for Ag[30]/SiO_2[31]/Si@25 °C, and Ag[30]/SiO_2[110]/Si@25 °C, fitting results exhibit an S parameter of about 0.9 in Ag overlayer. It should be noted that the positron diffusion length L_+ in Ag overlayer fitted from VEPFIT is around 9 nm, which is much shorter than that in Ag single crystal (about 110 nm) [32], indicating the presence of structural defects in Ag overlayer which trap positrons and reduce the diffusion length. In the low energy region ($E < 2$ keV) of the S-*E* curves, the S parameter decreases with increasing positron incident energy. The initial points in the two curves of Ag[30]/SiO_2[30]/Si@25 °C and Ag[30]/SiO_2[110]/Si@25 °C show the relative high values of S parameter, which is most probably due to the higher S parameter in the surface state. The depth-resolved analysis of the S-*E* curve by VEPFIT program can thus clearly identify the Ag overlayer, SiO_2 layer, SiO_2/Si interface and Si substrate for the samples deposited at 25 °C.

The S-*E* curves measured for all the Ag/SiO_2/Si multilayers grown at different substrate temperatures are shown in Fig. 4. At the first glance, it could be easily found that the two SiO_2/Si samples without Ag films have much higher S parameter than that of all Ag/SiO_2/Si, especially in the low energy region of less than 3.6 keV (corresponds to the mean implantation depth of 30 nm in Ag or 120 nm in SiO_2). In this figure, for the five samples with T_{sub} higher than 25 °C (Ag[30]/SiO_2[31]/Si@200, 400, and 600 °C; and Ag[30]/SiO_2[110]/Si@300 and 600 °C), the S-*E*

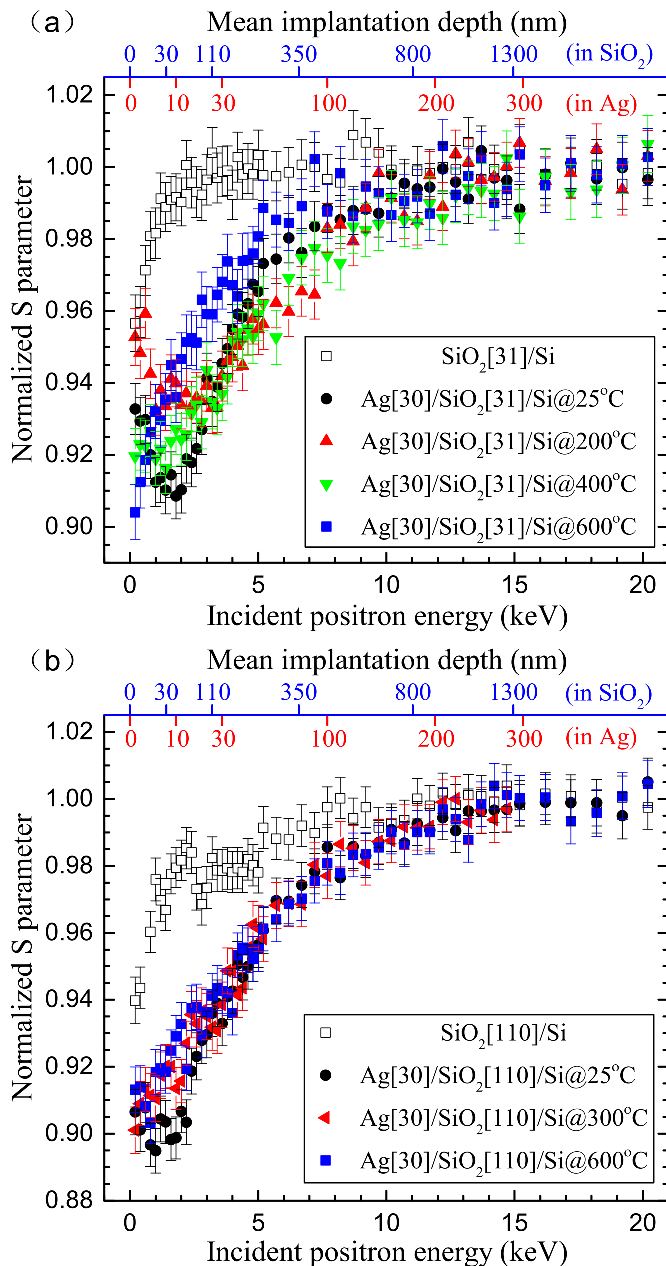

Fig. 4. Normalized S parameter as a function of incident positron energy for (a) Ag[30]/SiO_2[31]/Si samples that deposited at different T_{sub} and (b) Ag[30]/SiO_2[110]/Si samples that deposited at different T_{sub}.

curves cannot be well fitted by VEPFIT. This is most probably due to the destruction of the multilayer structure. It is suggested that Ag atoms get enough kinetic energy to diffuse through the SiO_2 layer at higher T_{sub}. This diffusion process plays a critical role for epitaxial growth of Ag on oxide-covered Si.

Compared to Ag[30]/SiO_2[31]/Si@25 °C, Ag[30]/SiO_2[31]/Si@200 °C shows a much higher S parameter in the energy region below 4 keV but a lower S parameter between 4 and 8 keV. From depth-resolved XPS analysis, we know that, with increasing T_{sub}, some fraction of Ag atoms penetrate into SiO_2 layer. Thus, the multilayer structure is destroyed and the measured S parameter of Ag[30]/SiO_2[31]/Si@200 °C is a weighted average of both Ag and SiO_2 in the low energy stage since positron diffusion length in either Ag (around 9 nm) or SiO_2 (less than 5 nm) is very short. The situation in Ag[30]/SiO_2[31]/Si@400 °C is similar to that deposited at 200 °C. In the energy region of $E > 4$ keV, these two curves are nearly the same. However, the S-*E* curve of Ag[30]/SiO_2[31]/Si@600 °C demonstrates a totally different shape. In the low energy region ($E < 7$ keV), the S parameter increases monotonically with increasing positron energy, and in the high energy region ($E > 7$ keV), the S-*E* curve is just the same as that of SiO_2[31]/Si. At T_{sub} = 600 °C, energetic Ag atoms not only penetrate into SiO_2 layer but also induce desorption of SiO_2 layer so that much of the Ag atoms were deposited directly on the surface of Si substrate. This is confirmed by the XPS measurements mentioned above. The XRD φ-scan profiles also confirm the epitaxial growth of Ag films on the Si substrate.

For Ag[30]/SiO_2[110]/Si samples grown at higher T_{sub}, which is shown in Fig. 4b, the penetration of Ag atoms into SiO_2 layer can still be observed from S-*E* curves and the situations in these cases are very similar to that in Ag[30]/SiO_2[31]/Si samples. The Ag[30]/SiO_2[110]/Si@300 °C and 600 °C samples have higher S values in the low energy region than that deposited at 25 °C. This is certainly the consequence of Ag diffusing into SiO_2 layer. However, a 110-nm-thick SiO_2 layer is rather difficult for Ag atoms to penetrate through and reach the Si surface, so the difference between Ag[30]/SiO_2[31]/Si@600 °C and Ag[30]/SiO_2[110]/Si@600 °C is evident. In Ag[30]/SiO_2[31]/Si@600 °C, the thickness of SiO_2 layer is possible for the Ag atoms to reach Si substrate. However, the penetration of SiO_2 layer in Ag[30]/SiO_2[110]/Si@600 °C becomes difficult because the SiO_2 layer is much thicker.

4. Conclusion

To summarize, we investigated the Ag/SiO_2/Si system using depth-resolved slow positron beam together with XRD and depth-resolved XPS measurements. It is found that, at T_{sub} = 25 °C, the deposition of Ag on SiO_2/Si substrate will form Ag/SiO_2/Si multilayer structure with structural defects in Ag overlayer. As T_{sub} increases, energetic Ag atoms can penetrate into SiO_2 layer and drive SiO_2 layer out from Si substrate. At T_{sub} = 600 °C, the 31-nm-thick SiO_2 layer was nearly desorbed from Si surface as a result of Ag diffusion process, and the epitaxial growth of Ag films on Si substrate was obtained. While for Ag[30]/SiO_2[110]/Si, the 110-nm-thick SiO_2 layer is too thick to be penetrated through by Ag. It is expected that with thinner SiO_2, it could be much easier for Ag atoms to penetrate and further lead to epitaxial growth on Si surface.

Acknowledgments

This work was financially supported by the National Natural Science Foundation of China under Grant Nos. 11875248 and11775215. We would like to thank A. Kawasuso, M. Maekawa, and A. Miyashita (the National Institutes for Quantum and Radiological Science and Technology, Japan) for some experiments and helpful discussions.

References

[1] G. LeLay, Surf. Sci. 132 (1983) 169–204.
[2] A. Romanyuk, R. Steiner, D. Mathys, V. Thommen, P. Oelhafen, Surf. Sci. 602 (2008) L49–L52.
[3] V. Grazhulis, Prog. Surf. Sci. 36 (1991) 89–175.
[4] J.H. Je, T.S. Kang, D.Y. Noh, J. Appl. Phys. 81 (1997) 6716–6722.
[5] P. Kocán, P. SobotíK, I. Ošt'ádal, M. Kotral, Phys. Rev. B 69 (2004) 165409.
[6] T. Tanikawa, I. Matsuda, T. Nagao, S. Hasegawa, Surf. Sci. 493 (2001) 389–398.
[7] Y.W. Kim, N.G. Park, W.S. Cho, K.H. Chae, C.N. Whang, K.S. Kim, S.S. Kim, D.S. Choi, Surf. Sci. 396 (1998) 295–303.
[8] A. Romanyuk, R. Steiner, I. Mack, P. Oelhafen, D. Mathys, Surf. Sci. 601 (2007) 1026–1030.
[9] A. Samsavar, E.S. Hirschorn, F.M. Leibsle, T.-C. Chiang, Phys. Rev. Lett. 63 (1989) 2830–2833.
[10] D.C. Mckenna, G.C. Wang, K. Rajan, J. Electron. Mater. 20 (1991) 753–758.
[11] C. Khare, J.W. Gerlach, C. Patzig, B. Rauschenhach, Appl. Surf. Sci. 258 (2012) 9617–9622.
[12] T.-B. Hur, H.K. Kim, D. Perello, M. Yun, A. Kulovits, J. Wiezorek, J. Appl. Phys. 103 (2008) 103507.
[13] T.-B. Hur, H.K. Kim, J. Blachere, Phys. Rev. B 75 (2007) 205306.
[14] P. Kocán, I. Ošt'ádal, P. Sobotík, Surf. Sci. 600 (2006) 3928–3931.
[15] M.J. Puska, R.M. Nieminen, Rev. Mod. Phys. 66 (1994) 841–897.
[16] P.J. Shultz, K.G. Lynn, Rev. Mod. Phys. 60 (1988) 701–779.

[17] B. Nielsen, K.G. Lynn, D.O. Welch, T.C. Leung, G.W. Rubloff, Phys. Rev. B 40 (1989) 1434–1437.
[18] B. Nielsen, K.G. Lynn, Y.-C. Chen, D.O. Welch, Appl. Phys. Lett. 51 (1987) 1022–1023.
[19] P. Asoka-Kumar, K.G. Lynn, T.C. Leung, B. Nielsen, X.Y. Wu, J. Appl. Phys. 69 (1991) 6603–6606.
[20] P. Asoka-Kumar, K.G. Lynn, D.O. Welch, J. Appl. Phys 76 (1994) 4935–4982.
[21] F. Tuomisto, I. Makkonen, Rev. Mod. Phys. 85 (2013) 1583–1631.
[22] J. Mitroy, G.G. Ryzhikh, J. Phys. B: At. Mol. Opt. Phys. 32 (1999) L411–L417.
[23] J. Mitroy, M.W.J. Bromley, G.G. Ryzhikh, J. Phys. B: At. Mol. Opt. Phys. 35 (2002) R81–R116.
[24] G. Ryzhikh, J. Mitroy, J. Phys. B: At. Mol. Opt. Phys. 31 (1998) 5013–5022.
[25] X. Cheng, D. Babikov, D.M. Schrader, Phys. Rev. A 83 (2011) 032504.
[26] V.A. Dzuba, V.V. Flambaum, C. Harabati, Phys. Rev. A 62 (2000) 042504.
[27] V.A. Dzuba, V.V. Flambaum, Phys. Rev. Lett. 105 (2010) 203401.
[28] A. van Veen, H. Schut, M. Clement, J. de Nijs, A. Kruseman, M. Ijpma, Appl. Surf. Sci. 85 (1995) 216–224.
[29] Z.Q. Chen, A. Uedono, A. Ogura, H. Ono, R. Suzuki, T. Ohdairac, T. Mikado, Appl. Surf. Sci. 194 (1-4) (2002) 112–115.
[30] A. Stirling, A. Pssquarello, J.-C. Charlier, R. Car, Phys. Rev. Lett. 85 (2000) 2773–2776.
[31] E.H. Poindexter, P.J. Caplan, Prog. Surf. Sci. 14 (1983) 201–294.
[32] E. Soininen, H. Huomo, P.A. Huttunen, J. Makinen, A. Vehanen, P. Hautojärvi, Phys. Rev. B 41 (1990) 6227–6233.